

9828986

**International Symposium on Polymer Electrolytes
(XII: 29 August - 3 September 2010: Padova, Italy)**

- 1. PMMA-LiBOB gel electrolyte for lithium ion batteries, by M.Z. Kufian, S.N.F. Yusuf, S.R. Majid and A.K.Arof.**
- 2. Preparation and characterization of magnesium ion gel polymer electrolytes for application in electrical double layer capacitors, by M.Z. Kufian, A.A.S. Nabila, S.R. Majid and A.K. Arof.**
- 3. Characteristics of plasticized PEMA/PVdF-HFP blend polymer electrolyte films doped with lithium triflate salt in electrochromic device, by L.N. Sim, S.R. Majid and A.K. Arof.**

Perpustakaan Universiti Malaya



A515110955

PMMA-LiBOB Gel Electrolyte for lithium Ion Batteries

M.Z. Kufian, S.N.F. Yusuf, S.R. Majid, A.K. Arof*

Center for Ionics University of Malaya, Department of Physics, University of Malaya, 50603

Kuala Lumpur, Malaysia

*Corresponding Author: akarof@um.edu.my

Tel: +603-79674085

Fax: +603- 79674146

ABSTRACT

Different amounts of lithium bis(oxalate) borate (LiBOB) have been added into a mixture of equal amounts of ethylene carbonate (EC) and propylene carbonate (PC) by weight. The highest conducting liquid electrolyte is 0.6 M LiBOB in EC/PC with room temperature conductivity of $4.1 \times 10^{-3} \text{ S cm}^{-1}$. Different amounts of PMMA are then added to this composition and heated between 70-80 °C for 20 min to obtain gel polymer electrolytes. The sample containing 18.67 wt.% PMMA was chosen for characterization and fabrication of lithium ion battery. Transference number measurements for lithium ion from Bruce-Vincent and DC polarization methods are 0.26 and 0.22, respectively. Linear sweep voltammetry indicates that the gel electrolyte decomposition voltage is approximately 4.7 V. Cyclic voltammetry shows an anodic peak at 1.30 V, 1.31 V and 2.45 V vs Li at a scan rate of 1, 5 and 7.5 mVs⁻¹, respectively, indicating decomposition of LiBOB. Battery performance over 20 cycles shows discharge capacity of about 130 mAhg⁻¹.

Keywords: Gel electrolyte, PMMA, LiBOB

1. INTRODUCTION

Much attention has been paid to gel electrolytes since liquid electrolytes pose many problems such as solvent vaporization, electrochemical corrosion and leakage. Conductivity of gel electrolytes can be as high as $10^{-3} \text{ S cm}^{-1}$ at room temperature. Using gel electrolytes, good electrode-electrolyte interfacial contact can be maintained during the battery cycling [1].

A great number of lithium salts have been extensively studied for its application in lithium ion batteries. These include LiAsF_6 [2], which is highly toxic, LiClO_4 [3] that gives excellent conductivity, but difficult to handle, LiBF_4 [4], which tends to produce a solid electrolyte interphase (SEI) layer of bad quality, LiCF_3SO_3 that produces electrolytes with quite low conductivity and $\text{LiN}(\text{SO}_2\text{CF}_3)_3$ and $\text{LiC}(\text{SO}_2\text{CF}_3)_3$ that can corrode the aluminium current collector. Research has focused on a different lithium salt based on a chelated borate anion namely, lithium bis(oxalate) borate or LiBOB. LiBOB consists of a large anion with delocalized charge [5]. LiBOB is non-toxic, low cost and has wide electrochemical window and high thermal stability [5-10]. LiBOB is stable until 302°C . LiPF_6 that is being used in commercial batteries is comparatively less stable at high temperatures and decomposes to LiF and PF_5 [11-14]. This can result in electrode passivation and poor battery performance. LiBOB has been actively used as a doping salt in a number of polymer electrolytes systems. LiBOB has doped in a blend of PVC and PVdF by Arivandan et al. [14] resulting in a conductivity of $5 \times 10^{-6} \text{ S cm}^{-1}$. When doped in PEO [5], the maximum conductivity obtained is of the order $10^{-5} \text{ S cm}^{-1}$. A conductivity of 4.22×10^{-4} has been reported by Reiter et al. [15] when LiBOB was doped in poly(2-ethoxyethyl methacrylate), PEOEMA. The presence of methacrylate in PEOEMA led us to use poly(methylmethacrylate), PMMA in this work. Methacrylate-based electrolyte exhibits high electrochemical stability, which allows their application in lithium ion batteries [15]. PMMA

has high boiling point (473 K), good impact strength, easy to dissolve and has excellent environmental stability. Ramesh et al. [16] reported a conductivity of $9.88 \times 10^{-5} \text{ S cm}^{-1}$ for PMMA doped with LiCF_3SO_3 . Ali et al. [17] reported a maximum conductivity of $1.25 \times 10^{-4} \text{ S cm}^{-1}$ for PMMA- $\text{LiN}(\text{CF}_3\text{SO}_2)_2$ system. Conductivity of $\sim 10^{-3}$ and $\sim 10^{-4} \text{ S cm}^{-1}$ were obtained when PMMA was doped with LiClO_4 and LiAsF_6 , respectively [18-19].

In this work, gel polymer electrolytes have been prepared with PMMA as the polymer host and LiBOB as the doping salt. A mixture of ethylene carbonate (EC) and propylene carbonate (PC) in a 1:1 weight ratio is the solvent. The performance of the PMMA-EC-PC-LiBOB as a separator/electrolyte in lithium batteries is presented and discussed.

2. EXPERIMENTAL

2.1 Preparation of liquid electrolytes

Different amounts of LiBOB were introduced into the EC:PC (1:1) to prepare liquid electrolytes with concentration 0.2, 0.4, 0.6, 0.8, and 1.0 M LiBOB in EC/PC (w/w = 1). The mixtures were stirred for 24 h to obtain homogeneous solutions.

2.2 Preparation of gel electrolyte

Five samples of gel electrolyte were prepared. 12.4 mL of propylene carbonate and 11.4 mL ethylene carbonate were mixed together and stirred for about 30 min. 2.67 g of LiBOB was added to the homogeneous EC/PC solution (equivalent to 0.6 M LiBOB in EC/PC) with continuous stirring for another 3 h. Different amounts of PMMA (9.25 wt. %, 18.67 wt. %, 28.24

wt. %, 37.97 wt. %, and 47.87 wt. %) were added to the 0.6 M LiBOB liquid electrolyte. All the solutions were cast into glass petri dishes and heated between 70 to 80° C for 20 min.

2.3 Samples characterization

2.3.1 Electrochemical Impedance Spectroscopy

EIS measurements were performed using HIOKI 3531 Z Hitester, in the frequency range between 50 Hz to 1 MHz. The films were sandwiched between two stainless steel disc electrodes. The impedance data are presented in a complex impedance plot where the imaginary part, Z_i of impedance was plotted against its real part, Z_r . From the plot, with the horizontal and vertical axes having the same scale, the bulk resistance, R_B can be obtained. The electrical conductivity, σ of the sample can be calculated using this equation,

$$\sigma = \frac{t}{R_b A}$$

where t is the thickness of the sample and A is the area of the sample.

2.3.2 Transference number measurement

2.3.2.1 Bruce-Vincent Method

A constant DC potential (10 mV) was applied across a symmetrical Li/GPE/Li cell. The current was monitored as a function of time until it reached a constant value. AC impedance spectroscopy was carried out before and after the applied voltage pulse to estimate the effect of charge conduction through the passivating layer at the electrode–electrolyte interface.

2.3.2.2 DC Polarization Method

In this technique, the DC current is monitored as a function of time on application of fixed DC voltage across the sample with electrode. In this study, stainless steel and lithium metal were used as blocking and non-blocking electrode respectively. 10 mV DC was used as applied voltage.

2.3.2.3 Solid electrolyte interphase (SEI) layer

In order to determine the thickness of the SEI layer a Li/GPE/Li cell was assembled in a glove box with argon environment. The cell was stored at 60 °C for about 24 hours and the impedance of the cell was measured using HIOKI 3531 Z Hi tester in the frequency range between 50 Hz to 1 MHz with applied voltage of 0.5 V. This step was repeated until the interfacial resistance of the GPE cell was constant. The thickness of the SEI layer can be calculated using equation below:

$$l = \omega_{\max} \epsilon_0 \epsilon_r AR$$

where l = thickness of the SEI layer, ϵ_0 = permittivity of vacuum, ϵ_r = permittivity of lithium-based materials which is taken as 10 [20]. A is area of the electrode and R is measured resistance.

2.3.3 Linear Sweep Voltammetry and Cyclic Voltammetry

Samples have been characterized by linear sweep voltammetry (LSV) and cyclic voltammetry (CV) in order to investigate the electrochemical behavior of the polymer electrolyte. LSV and CV measurements were performed by using Electrochemical Analyzer Autolab. For both methods, nickel plates were used as working electrodes while lithium metals were used as reference and counter electrodes. LSV was done at scan rate of 5 mV s⁻¹.

A515110955

2.3.4 Battery Fabrication and characterization

In this work, lithium half-cells were fabricated using lithium cobalt oxide, LiCoO_2 and lithium foil as cathode and anode respectively. The cathode (LiCoO_2 as the active material) was coated on aluminium foil. The cathode film was punched into small discs with an effective electrode area of 2.27 cm^2 and dried at 110°C under vacuum for 16 h before use. GPE was used as the separator and sandwiched between the cathode and anode. The cells were fabricated by packing in CR 2032 coin cell. The theoretical capacity of the cell is 130 mAh g^{-1} . The cells were characterized at constant charge-discharge current (1 mA) at room temperature. Charge-discharge measurements and cycling tests were carried out using Neware battery cycler.

3 RESULTS AND DISCUSSIONS

3.1 Electrochemical Impedance Spectroscopy

The variation of room temperature conductivity for liquid electrolytes with different molarities of LiBOB in EC and PC is shown in Figure 1. It is observed that the conductivity of 0.2 M LiBOB salt in EC:PC (1:1) is $2.7 \times 10^{-3} \text{ S cm}^{-1}$. The conductivity further increases until the maximum value of $4.1 \times 10^{-3} \text{ S cm}^{-1}$ for the 0.6 M LiBOB liquid electrolyte. This is attributed to the increase in the number density of free ions as the salt concentration increases. However, on addition of more LiBOB salt, the conductivity begins to decrease and drops to $\sim 3.7 \times 10^{-3} \text{ S cm}^{-1}$ at 0.8 M. After the optimum concentration, an increase in salt concentration results in higher ion aggregation and higher viscosity of the solution, which reduces the free-ion number and the ionic mobility, respectively [21], leading to the decrease in conductivity.

Figure 1: Effects of LiBOB concentration on the conductivity at room temperature.

The room temperature conductivity of the gel polymer electrolytes as a function of polymer concentration is shown in Figure 2. Sample with the lowest concentration of PMMA, 9.25 wt. % gives the maximum conductivity with $3.93 \times 10^{-4} \text{ S cm}^{-1}$. As the concentration of PMMA increases, the conductivity is observed to decrease. Polymer electrolyte containing 47.87 wt. % of PMMA shows the lowest conductivity value of $4.75 \times 10^{-5} \text{ S cm}^{-1}$. The sample is also observed to be too hard, while the highest conducting 9.25 wt. % PMMA polymer electrolyte is wet. Thus, the polymer electrolyte containing 18.67 wt. % of PMMA with conductivity value of $2.51 \times 10^{-4} \text{ S cm}^{-1}$ is chosen for further investigations.

Figure 2: Variation of conductivity of PMMA-LiBOB electrolyte as a function of PMMA concentration

It is known that the ionic conductivity of gel polymer electrolytes is strongly dependent on temperature. Figure 3 shows temperature dependence of ionic conductivity for PMMA-LiBOB electrolyte at two different compositions of PMMA. Gel electrolyte sample with 18.67 wt. % PMMA-LiBOB shows better temperature dependence than 47.87 wt. % PMMA-LiBOB. Activation energy values, E_A , exhibited in Table 1, were obtained from the Arrhenius equation as shown below:

$$\sigma = \sigma_0 e^{-\frac{E_A}{kT}}$$

where σ_0 is the pre-exponential factor and k is Boltzman's constant. E_A is the most important parameter that determines the variations of polymer electrolyte conductivity with temperature. From Table 1, we can see that the activation barrier appears to increase with increasing PMMA content. These results support the conductivity plot in Figure 3, where, as the PMMA content increases the conductivity drops due to the higher viscosity [1] in the vicinity of the ions.

Table 1: Activation energy and regression values of the electrolyte

PMMA/ wt. %	E_A/eV	R^2
9.25	0.1975	0.900
18.67	0.1980	0.963
28.24	0.2352	0.915
37.97	0.2357	0.903
47.87	0.2251	0.922

Figure 3: Temperature dependence of ionic conductivity of 18.67 wt. % and 47.87 wt. % PMMA gel electrolyte

3.2 Transference number

Figure 4 shows the polarization current curve for the highest conducting LiBOB based PMMA gel electrolyte film and the inset graph shows the impedance plot of the cell before and after DC pulse at 298 K. According to Bruce and Vincent [22], the lithium transference number, number can be calculated using the following equation:

$$t_{Li^+} = \frac{I_{ss} (\Delta V - I_o R_o)}{I_o (\Delta V - I_{ss} R_{ss})}$$

Here I_o is the initial current (at $t=0$), I_{ss} the steady state current, ΔV is applied voltage bias, and R_o and R_{ss} are the initial and final resistances of passive layer onto lithium metal electrodes. Following this method, $I_o = 1.68 \times 10^{-3}$ A, $\Delta V = 10$ mV, $I_{ss} = 3.78 \times 10^{-4}$ A, $R_o = 672 \Omega$ and $R_{ss} = 2550 \Omega$.

Figure 4: DC polarization curve for the highest conducting LiBOB-based PMMA gel electrolyte

DC polarization method

Figure 5 shows the polarization current plot as a function of time. The transference number is calculated using the equation:

$$t_{BOB^-} = \frac{(I_o - I_s)}{I_o}$$

where I_o is the initial current and I_s is the steady- state current. $t_{Li^+} = 1 - t_{BOB^-}$

Figure 5: Graph of polarization current versus time

The calculated lithium transport number, t_{Li^+} data are given in Table 2.

Table 2: t_{Li^+} transport number from different method

Method	t_{Li^+}
Bruce and Vincent	0.26
DC polarization	0.22

Since the I_s for SS/GPE/SS is very low, 4.06×10^{-7} A, i.e. $t_{electron} \sim 0.01$ the GPE is an ionic conductor. On changing the electrode to Li/GPE/Li, $I_o = 1.08 \times 10^{-3}$ A, $I_s = 3.78 \times 10^{-4}$ A and t_{Li^+} is 0.22.

3.3 Solid electrolyte interphase (SEI)

To the best of our knowledge, there no reports on the thickness of the SEI layer between the lithium metal electrodes and gel polymer electrolyte using LiBOB salt. Figure 6 shows the Cole – Cole plot of Li/GPE/Li for various times at 60 °C. The highest conducting sample PMMA-LiBOB gel electrolyte was used in these studies. The impedance of Li/ GPE / Li

increases with time. The change in impedance is due to the formation of the SEI layer between the electrolyte and electrodes [23].

Figure 6: Cole – Cole plot of Li/GPE/Li at various time at 60 °C.

The impedance of Li/GPE/Li cell was almost constant after 60 hours and attained the value 84 Ω . Sloop et al., reported the impedance remain constant at 100 Ω for Li/XPEM₂₄LiClO₄/Li cell [23]. Figure 7 showed the interfacial resistance, R_i versus time. The thickness of the SEI was calculated to be 1.6 Å .

Figure 7: Interfacial resistance as a function of time for the highest conducting sample

Result from linear sweep voltammetry is shown in Figure 8. The current density starts to increase dramatically when the potential exceeds 4.5 V. Decomposition of the electrolyte takes place at 4.7 V. Appetecchi et. al [24], reported the anodic break-down voltage for PMMA-EC-PC based electrolyte doped with LiClO₄, LiAsF₆ and LiN(CF₃SO₃)₂ is 4.6 V, 4.8 V and 4.8 V respectively. The decomposition voltage obtained from our PMMA-EC-PC-LiBOB electrolyte system lies closely with the PMMA-EC-PC polymer electrolytes reported in the literature.

Figure 8: LSV curve of PMMA-LiBOB polymer electrolyte

Figure 9: Cyclic Voltammogram for at (a) 1 mV s^{-1} , (b) 5 mV s^{-1} and (c) 7.5 mV s^{-1}

Figure 9 shows the cyclic voltammograms of 20 wt. % PMMA-80 wt. % (0.6 M LiBOB EC/PC (w/w=1)) at 1 mV s^{-1} , 5 mV s^{-1} and 7.5 mV s^{-1} . CV scanned at 1 mV s^{-1} shows peaks at 1.16 V and 2.41 V versus Li. Peaks are present at 2.01 V and 2.45 V vs Li for curve at 7.5 mV s^{-1} .

Work done by Wang et. al [25] obtained the decomposition voltage of LiBOB/EC/EMC (1:1, v:v) from 1.35 V to 0 V vs Li at the scan rate of 5 mV s^{-1} . In comparison with our work, the CV of the highest conducting gel electrolyte shows a peak at almost similar value 1.31 V vs Li on the reverse cycle. This peak is present at slight voltage variations in all voltammograms for other scan rates.

Figure 10: Plot voltage over capacity of Li/GPE/LiCoO₂ for (a) 1st, (b) 5th and (c) 20th cycles.

Figure 10 shows the capacity of Li/GPE/LiCoO₂ at room temperature environment. The first cycle of the cell give capacity about 131 mAh g^{-1} and 5th and 20th cycle the capacity give 134 mAh g^{-1} and 135 mAh g^{-1} respectively. The increase in cycle numbers increased the capacity of the cells. This may be due to the electrochemical interaction inside the lithium batteries cells.

The internal resistances of the cell were decreased with increasing the number of cycle as shown in Table 3.

Table 3: Internal resistances of the cell with different cycles

ACKNOWLEDGEMENTS

The author thank the Ministry of Malaysia for the BRIC grant provided.

Cycle	Internal resistance/ Ω
1	500
5	430
20	230

Figure 11 shows the capacity of the cell depend on the cycle number. For the 1st cycle to 10th cycle, the capacity of the cell is not stable and may be due to the SEI layer formation on the cathode side.

Figure 11: Graph capacity vs cycle number

4. CONCLUSIONS

The conductivity of liquid electrolyte dropped on addition of PMMA. The conductivity dropped from 4.05 mS cm^{-1} to 0.25 mS cm^{-1} . PMMA doped LiBOB is stable until 4.7 V which is suitable for lithium batteries. From the charge-discharge curves, the internal resistance of the cell is observed to decrease on cycling.

ACKNOWLEDGEMENTS

The author thanks the University of Malaya for the HIRG grant provided.

REFERENCES

- [1] G. P. Pandey, R. C. Agrawal, S. A. Hashmi, *J. Power Sources*, 190 (2009), 563.
- [2] T. Nakajima, M. Mori, V. Gupta, Y. Ohzawa, H. Iwata, *Solid State Sci.*, 4 (2002) 1385.
- [3] Y.W. Chen-Yang, Y.T. Chen, H.C. Chen, W.T. Lin, C.H. Tsai, *Polymer* 50 (2009) 2856.
- [4] J. Vondrak, M. Sedlarikova, J. Reiter, T. Hodal, *Electrochim. Acta* 44 (1999) 3067.
- [5] H. H. Sumathipala, J. Hassoun, S. Panero, B. Scrosati, *Ionics* 13 (2007) 281.
- [6] V. Aravindan, P. Vickraman, *Ionics* 13 (2007) 277.
- [7] J. Huang, L.Z. Fan, B. Yu, T. Xing, W. Qiu, *Ionics* 16 (2010) 509.
- [8] D. Moosbauer, S. Zugmann, M. Amereller, H. J. Gores, *J. Chem. Eng. Data* 55 (2010) 1794.
- [9] M. Amereller, M. Multerer, C. Schreiner, J. Lodermeier, A. Schmid, *J. Chem. Eng. Data* 54 (2009) 468.
- [10] W. Xu, L.-M. Wang, R.A. Nieman, and C.A. Angell, *J. Phys. Chem. B* 107 (2003) 11749.
- [11] S. Wang, W. Qiu, T. Li, B. Yu, H. Zhao, *Int. J. Electrochem. Sci.*, 1 (2006) 250.
- [12] L. Larush-Asraf, M. Biton, H. Teller, E. Zinigrad, D. Aurbach, *J. Power Sources* 174 (2007) 400.
- [13] W. Lu, Z. Chen, H. Joachin, J. Prakash, J. Liu, K. Amine, *J. Power Sources* 163 (2007) 1074.
- [14] V. Aravindan, P. Vickraman, T.P. Kumar, *J. Membr. Sci.* 305 (2007) 146.
- [15] J. Reiter, O. Krejza, M. Sedlarikova, *Solar Energy Materials & Solar Cells* 93 (2009) 249.

- [16] S. Ramesh, Koay Hang Leen, K. Kumutha, A.K. Arof, *Spectrochim. Acta* 66A (2007) 1237.
- [17] A.M.M. Ali, M.Z.A. Yahya, H. Bahron, R.H.Y. Subban, M.K. Harun, I. Atan, *Mater. Letts.* 61 (2007) 2026.
- [18] Hsien-Wei Chen, Tzu-Pin Lin, Feng-Chih Chang, *Polymer* 43 (2002) 5281.
- [19] S. Rajendran, T. Uma, T. Mahalingam, *Euro. Polym. J.* 36 (2000) 2617
- [20] A. M. Stephan, T. P. Kumar, M. A. Kulandainathan, N. .A. Lakshmi, *J. Phys. Chem. B* (113) 2009 1963
- [21] F. Azeez, P. S. Fedkiw, *J. Power Sources* 195 (2010) 7627.
- [22] P.G. Bruce, M.T. Hardgrave, C.A. Vincent, *Electrochim. Acta* 37 (1992) 1517.
- [23] S. E. Sloop, M. M. Lerner, *Solid State Ionics* 85 (1996) 251
- [24] G.B. Appetecchi, F. Croce, R. Marassi, L. Persi, P. Romagnoli, B. Scrosati, *Electrochim. Acta* 45 (1999) 23.
- [25] S. Wang, W. Qiu, T. Li, B. Yu, H. Zhoo, *Int. J. Electrochem. Sci.* 1 (2006) 250.

List of figures

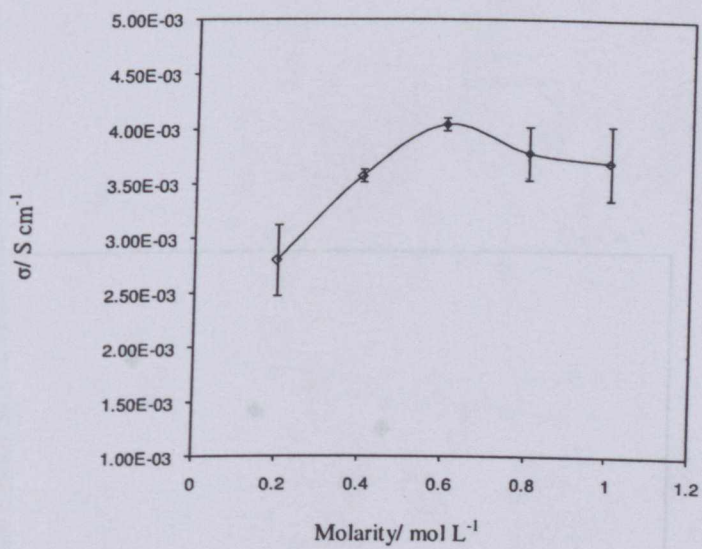


Figure 1

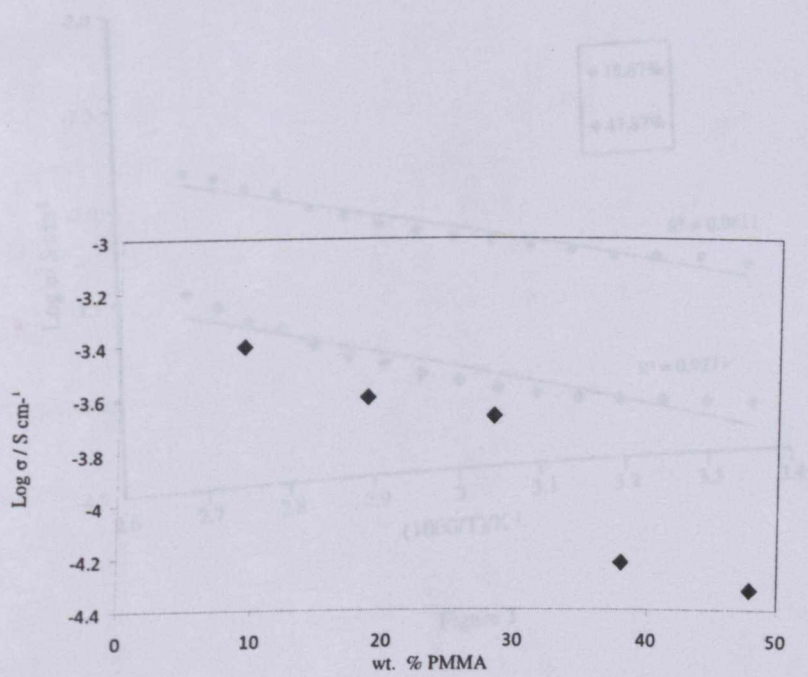


Figure 2

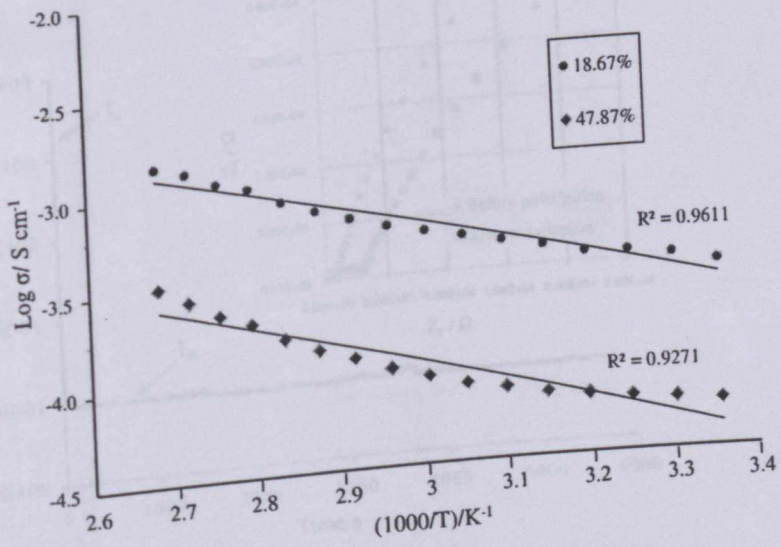


Figure 3

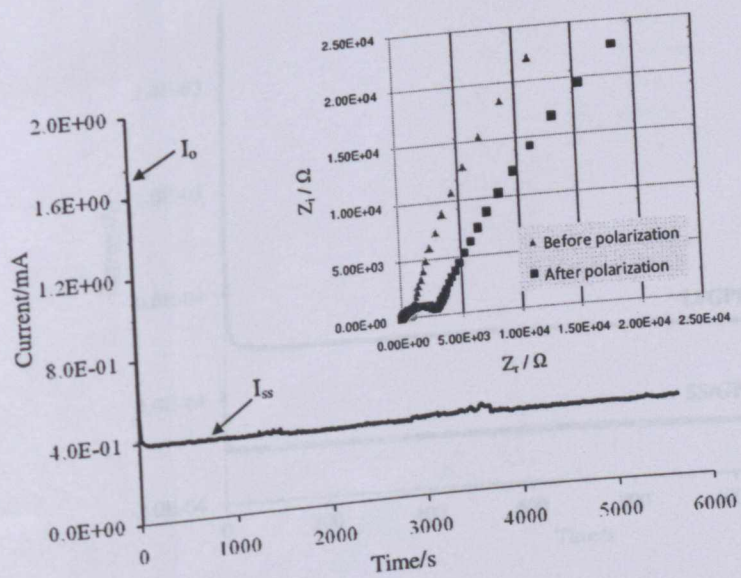


Figure 4

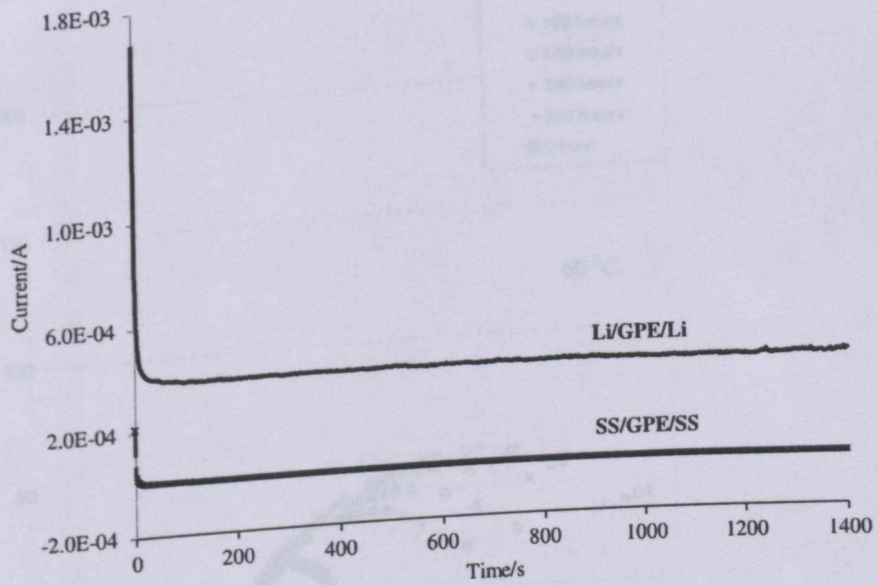


Figure 5

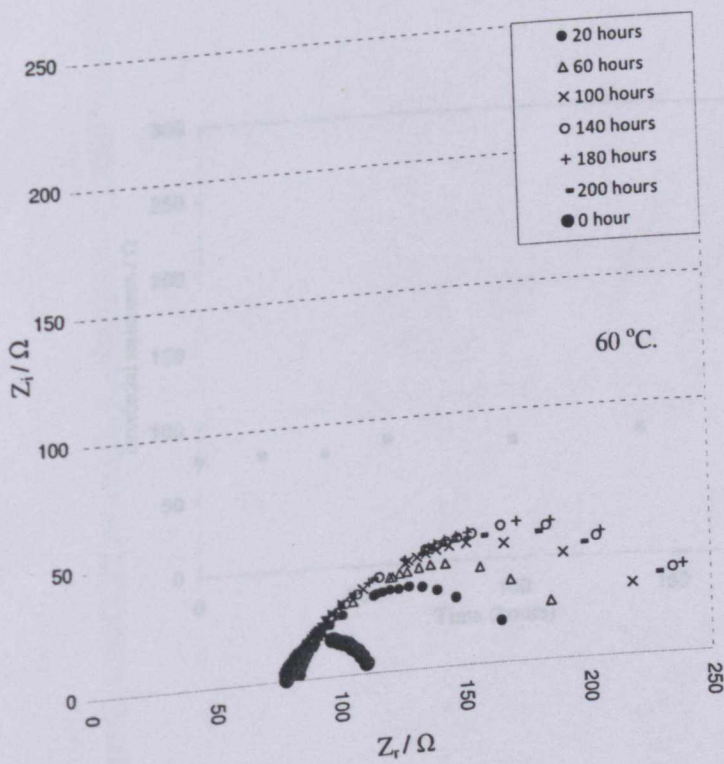


Figure 6

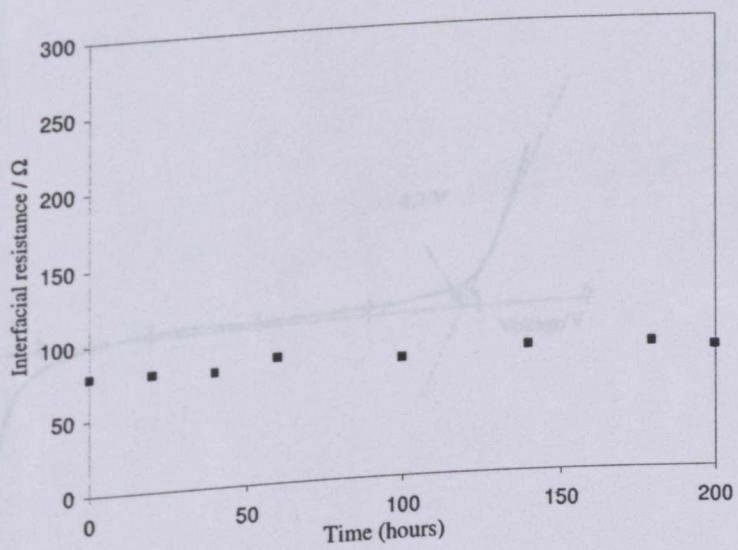


Figure 7

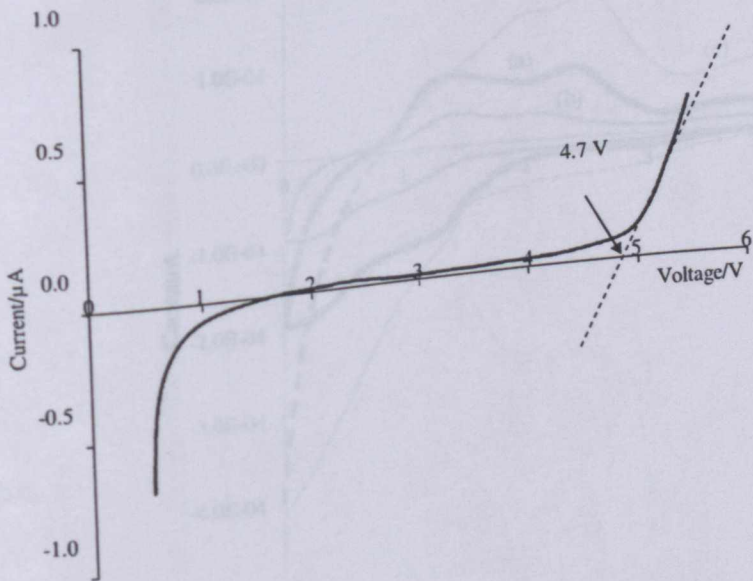


Figure 8

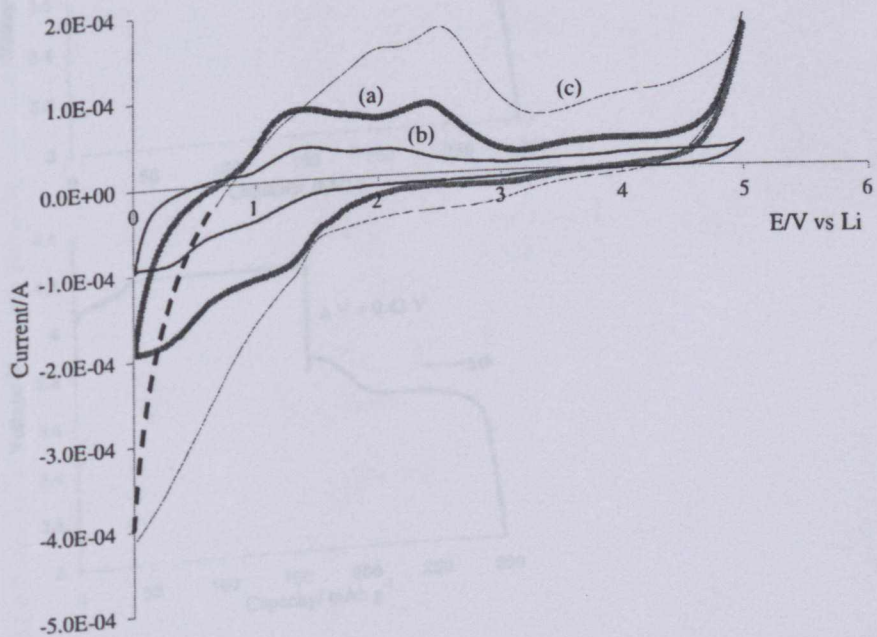


Figure 9

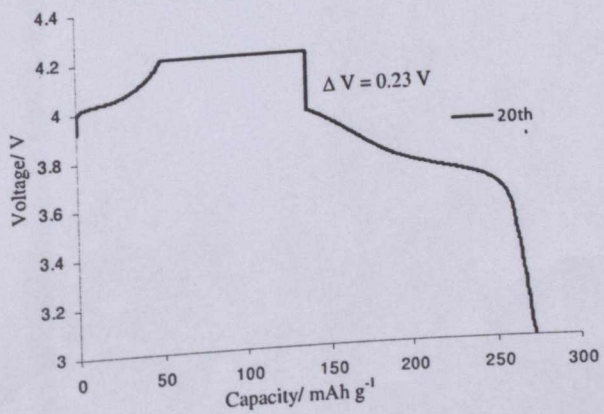
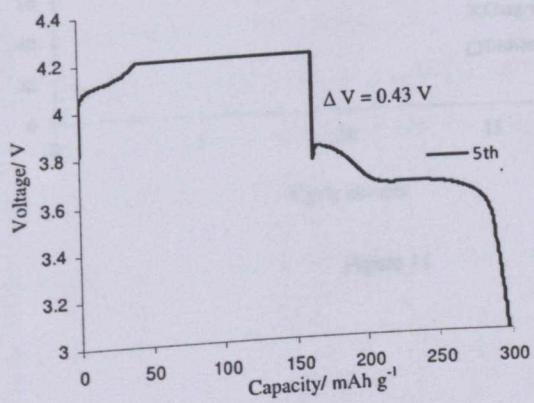
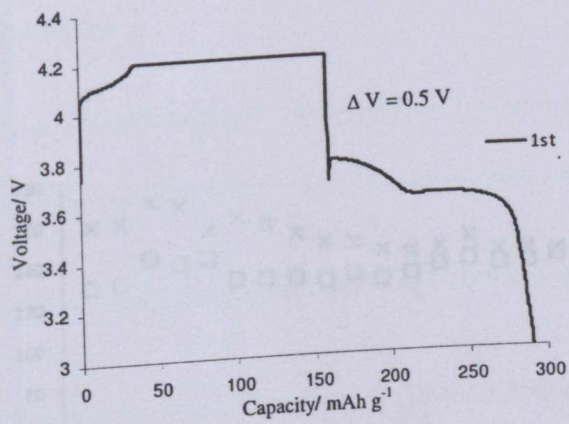


Figure 10

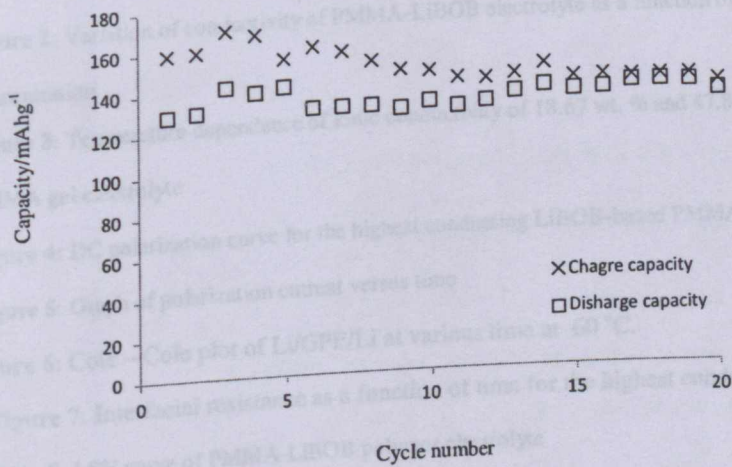


Figure 11

List of Figure captions

Figure 1: Effects of LiBOB concentration on the conductivity at room temperature.

Figure 2: Variation of conductivity of PMMA-LiBOB electrolyte as a function of PMMA concentration

Figure 3: Temperature dependence of ionic conductivity of 18.67 wt. % and 47.87 wt. % PMMA gel electrolyte

Figure 4: DC polarization curve for the highest conducting LiBOB-based PMMA gel electrolyte

Figure 5: Graph of polarization current versus time

Figure 6: Cole – Cole plot of Li/GPE/Li at various time at 60 °C.

Figure 7: Interfacial resistance as a function of time for the highest conducting sample

Figure 8: LSV curve of PMMA-LiBOB polymer electrolyte

Figure 9: Cyclic Voltammogram for at (a) 1 mV s⁻¹, (b) 5 mV s⁻¹ and (c) 7.5 mV s⁻¹

Figure 10: Plot voltage over capacity of Li/GPE/LiCoO₂ for (a) 1st, (b) 5th and (c) 20th cycles.

Figure 11: Graph capacity vs cycle number